

## Magnetron priming by multiple cathodes

M. C. Jones,<sup>a)</sup> V. B. Neculaes,<sup>b)</sup> Y. Y. Lau,<sup>c)</sup> R. M. Gilgenbach, W. M. White, B. W. Hoff, and N. M. Jordan

*Intense Energy Beam Interaction Laboratory, Department of Nuclear Engineering and Radiological Sciences, University of Michigan, Ann Arbor, Michigan 48109-2104*

(Received 2 May 2005; accepted 30 June 2005; published online 15 August 2005)

A relativistic magnetron priming technique using multiple cathodes is simulated with a three-dimensional, fully electromagnetic, particle-in-cell code. This technique is based on electron emission from  $N/2$  individual cathodes in an  $N$ -cavity magnetron to prime the  $\pi$  mode. In the case of the six-cavity relativistic magnetron,  $\pi$ -mode start-oscillation times are reduced up to a factor of 4, and mode competition is suppressed. Most significantly, the highest microwave field power is observed by utilizing three cathodes compared to other recently explored priming techniques. © 2005 American Institute of Physics. [DOI: 10.1063/1.2031928]

In the last 50 years, the magnetron<sup>1</sup> has become the most widespread microwave vacuum electronics device in the world. Reliability, ruggedness, and efficiency make magnetrons suitable for a wide range of commercial applications: microwave ovens, radar, industrial heating, medical accelerators, and plasma sources.<sup>2</sup> In the defense community, there exists significant interest in the research and development of relativistic magnetrons.<sup>3,4</sup>

While magnetron rf priming is a well-established method,<sup>5,6</sup> more innovative priming techniques have recently shown dramatic improvements in achieving fast oscillation startup, suppression of mode competition, rapid frequency stabilization, and noise reduction. Magnetic priming initiated the concept of modulating the  $E_0 \times B_0$  drift velocity of electrons by using an axial magnetic field with  $N/2$ -fold symmetry<sup>7-9</sup> in an  $N$ -cavity magnetron operating in the  $\pi$  mode. This  $E_0 \times B_0$  modulation has recently been obtained by introducing periodic anode shape modification (dc, radial, electric priming).<sup>10</sup> Cathode priming employs emission from  $N/2$  discrete zones around the azimuth of the cathode in an  $N$ -cavity magnetron operating in the  $\pi$  mode.<sup>11,12</sup> The space charge of the  $N/2$  electron bunches that are instantaneously formed in cathode priming might also have seeded the azimuthal (rf) electric field with an  $N/2$ -fold symmetry ( $\pi$  mode). This paper introduces a priming technique that uses  $N/2$  individual cathodes to prime the  $\pi$  mode in an  $N$ -cavity magnetron. This scheme appears to produce the highest microwave power among all recently proposed priming techniques.

Three-dimensional (3D) simulations of triple-cathode priming were performed in a six-cavity relativistic magnetron using a 3D particle-in-cell code, MAGIC.<sup>13</sup> The simulation geometry is shown in Fig. 1(a), which represents the baseline case with no priming (single cathode), and in Fig. 1(b), which represents the triple-cathode priming case. Three individual cathodes are required to prime the  $\pi$  mode in the six-cavity magnetron.<sup>14,15</sup> The simulated baseline configuration is based on the relativistic magnetron geometry in operation at the University of Michigan, which is reported elsewhere.<sup>11</sup> Extensive simulations were performed with the

baseline case [single cathode, Fig. 1(a)], and with triple-cathode configuration [Fig. 1(b)] with angular emission widths of 15°, 30°, 45°, 60°, 75°, and 90°. For each angular emission width, two simulations were performed, with the cathodes centered under the vanes versus under the cavities. Voltage was 300 kV (with a rise time of approximately two rf periods), magnetic field set to 3.0 kG, and the emission length was kept constant at 14 cm.

Other researchers have proposed a “transparent cathode,” in which a cathode with “many longitudinal bands” of an unspecified number cut along it,<sup>16</sup> in order to improve magnetron performance. Here, simulations with five (angular emission widths of 27°), seven (19.3°), and twelve cathodes (11°) have also been performed for comparison with the optimal three cathodes (equal to the number of electron spokes in the  $\pi$  mode in the six-cavity relativistic magnetron), in terms of startup, output power, and mode locking.

First, in contrast to cathode priming<sup>11,12</sup> and magnetic priming,<sup>7-9</sup> the cold test  $\pi$ -mode frequency changes with triple-cathode priming. Furthermore, variation of the angular emission width with three cathodes causes variation of the cold test  $\pi$ -mode frequency, as shown in Fig. 2, with the three cathodes centered under the vanes. The “hot” test  $\pi$ -mode frequency (when electrons are emitted) also varies with the angular emission width (Fig. 2).

The introduction of three separate cathodes produces a threefold symmetry in the electron cloud, which favors fast startup and  $\pi$ -mode locking. Figure 3 illustrates the dramatic effects with three cathodes, when the angular emission width

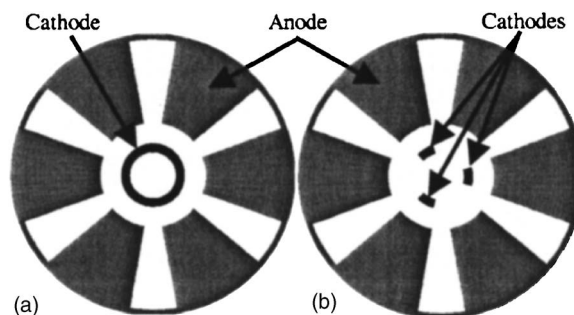


FIG. 1. Cross section of the simulated magnetron (a) with no triple-cathode priming and (b) with triple-cathode priming showing the three cathodes (30°) centered under the vanes.

<sup>a)</sup>Current address: Sandia National Laboratory, Albuquerque, NM.

<sup>b)</sup>Current address: General Electric Research Center, Niskayuna, NY.

<sup>c)</sup>Electronic mail: yylau@umich.edu

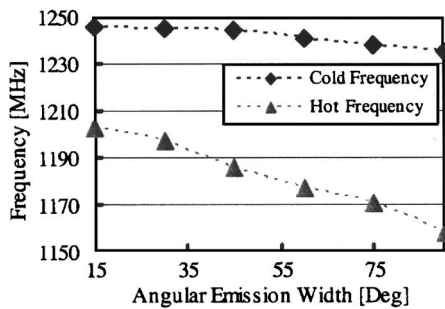


FIG. 2.  $\pi$ -mode frequency vs angular emission width for triple cathodes (centered under the anode vanes).

is set to  $30^\circ$ , centered under the cavities. At 3 ns, the electron hub with a single cathode is tightly packed around the cathode (a), whereas with three cathodes, the expanded electron cloud has already developed a threefold symmetry (b). Later, at 7 ns, the triple-cathode priming case exhibits three electron spokes interacting with the cavities, in stark contrast with the baseline, single cathode case (c). By 15 ns, the electron cloud develops two electron spokes, when no priming is applied (e), characteristic of the undesired  $2\pi/3$  mode, while with triple-cathode priming the three electron spokes remain locked in the  $\pi$  mode. Finally, at 25 ns, the baseline case (g) reaches stable  $\pi$ -mode operation, while with three cathodes the magnetron continues to be locked in stable  $\pi$ -mode operation (h).

The instantaneous frequency of the rf electric field measured at the center of a cavity versus time is presented in Fig. 4. Figure 4 illustrates very rapid ( $\sim 6$  ns)  $\pi$ -mode locking with triple-cathode priming. Note the large variation in the instantaneous frequency with a single cathode until 30 ns.

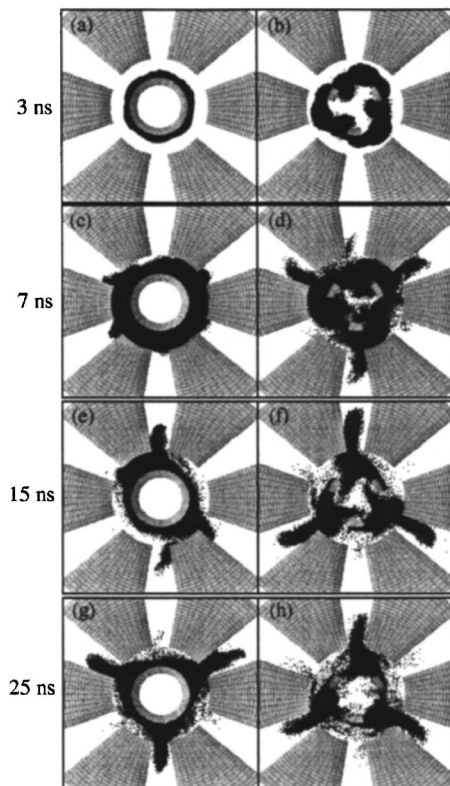


FIG. 3. Electron phase space plots for no cathode priming (a), (c), (e), and (g) and triple-cathode priming ( $30^\circ$  angular emission width under the cavities) (b), (d), (f), and (h).

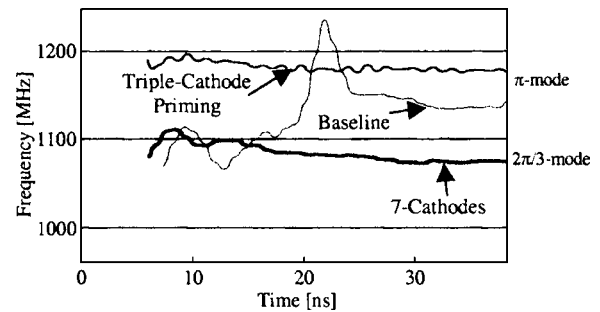


FIG. 4. Instantaneous frequency of rf electric field vs time for (a) no priming, (b) triple-cathode priming ( $30^\circ$  angular emission width centered under cavities), (c) seven cathodes.

For comparison, when seven cathodes are utilized, fast frequency stabilization is observed; however, the magnetron operates in the undesired  $2\pi/3$  mode. In addition, this  $2\pi/3$  mode exhibits a large field power loss compared with the baseline case (Fig. 5).

In contrast, triple-cathode priming demonstrates robust, rapid mode growth (Fig. 5), fast  $\pi$ -mode locking (Fig. 4), and a significant increase in rf power (field power measured at the back of a cavity). For the case presented in Fig. 5, ( $30^\circ$  angular emission widths centered under the cavities), magnetron rf power is 25% higher compared to the baseline, single cathode simulation. This increased power is unique to triple-cathode priming, and has not been observed in the experiments and simulations of magnetic priming<sup>8,17</sup> or of cathode priming.<sup>11,12</sup>

For each angular emission width ( $15^\circ$ ,  $30^\circ$ ,  $45^\circ$ ,  $60^\circ$ ,  $75^\circ$ , and  $90^\circ$ ) there exist certain favorable orientations (e.g., under anode vanes or cavities) that lead to increased rf power levels with three cathodes compared to the baseline case. Figure 6 shows the enhancements in the estimated magnetron electronic efficiency with triple-cathode priming, observed mainly with smaller angular widths (up to 34% for  $15^\circ$  emission width cathodes centered under the cavities), for both cases of cathodes under the vanes and under the cavities. Magnetron efficiency was calculated by dividing the field power measured at the back of a cavity by the input power. With angular emission widths up to  $45^\circ$  the estimated magnetron electronic efficiency increases to an average of 26% with three-cathodes compared to 17% in the baseline, single cathode case (Fig. 6). Small emission width in the  $N/2$  cathodes naturally favors prebunching with an  $N/2$  azimuthal symmetry<sup>18</sup> (the opposite limit being that the  $N/2$  cathodes have such a large emission width that they merge into one

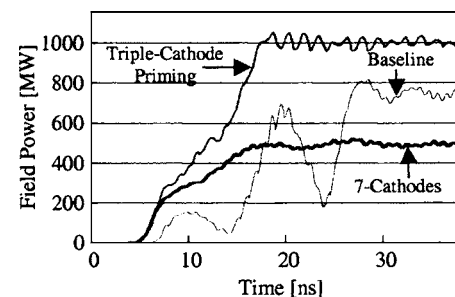


FIG. 5. Field power measured at back of a cavity vs time for (a) no priming, (b) triple-cathode priming ( $30^\circ$  angular emission width centered under cavities), (c) seven cathodes.

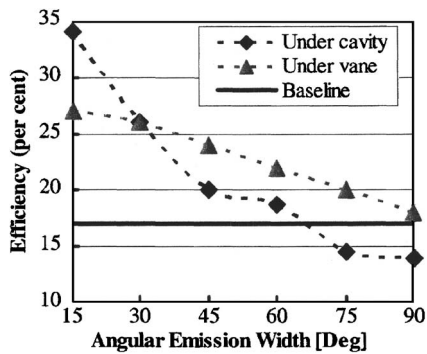


FIG. 6. Estimated magnetron electronic efficiency vs angular emission width. Also shown is the baseline case.

continuous cathode, in which case multiple-cathode priming is completely lost).

The above-noted simulations show that the frequency, output power, and efficiency in triple-cathode priming is sensitive to the orientation of the cathodes with respect to the anode block (e.g., centered under the vanes versus centered under the cavities). Therefore, this technique offers the interesting possibility of magnetron tuning: by simply rotating the triple-cathode structure with respect to the anode block, one could adjust the operating frequency, output power, and efficiency. In addition, the magnetron's impedance may be adjusted by varying the cathodes' angular width, thereby changing the dc current at a fixed operating voltage.

The five cathode case is similar to the baseline case in terms of  $\pi$ -mode startup time and field power. Twelve cathodes lock the six-vane magnetron in the  $2\pi/3$  mode, while considerably reducing the estimated output power (similar to the seven-cathode case discussed earlier). These results demonstrate the advantage of triple-cathode priming compared to the baseline, single cathode and the five-, seven-, or twelve-cathode configurations.

In conclusion, a priming technique is proposed, using  $N/2$  individual cathodes in an  $N$ -cavity magnetron operating in the  $\pi$  mode. This method, which represents a major departure from the traditional magnetron cathode design, is shown in simulations to produce fast startup, rapid  $\pi$ -mode

growth,  $\pi$ -mode locking (suppression of mode competition), and potential for higher output power and efficiency. Finally, this investigation reveals several advantages of triple-cathode priming, even compared with the more recent concepts of magnetic priming and cathode priming.

This research was supported by AFOSR and by the AFOSR/MURI Program on Breakdown and Emission in High Power Microwave Sources. The authors appreciate AFOSR support of the MAGIC Users Group administered by Mission Research Corporation.

- <sup>1</sup>G. B. Collins, *Microwave Magnetron* (McGraw Hill, New York, 1948).
- <sup>2</sup>J. M. Osepchuk, *IEEE Trans. Microwave Theory Tech.* **50**, 975 (2002).
- <sup>3</sup>R. W. Lemke, T. C. Genoni, and T. A. Spencer, *IEEE Trans. Plasma Sci.* **28**, 887 (2000).
- <sup>4</sup>M. R. Lopez, R. M. Gilgenbach, M. C. Jones, W. M. White, D. W. Jordan, M. D. Johnston, T. S. Strickler, Y. Y. Lau, T. A. Spencer, M. D. Haworth, K. L. Cartwright, P. J. Mardahl, J. W. Luginsland, and D. Price, *IEEE Trans. Plasma Sci.* **32**, 1171 (2004).
- <sup>5</sup>H. Sze, R. R. Smith, J. N. Benford, and B. D. Harteneck, *IEEE Trans. Electromagn. Compat.* **34**, 235 (1992).
- <sup>6</sup>J. Robinson, M. Doherty, B. Davenport, M. Lander, and T. Treado, *Proceedings of the Third International Vacuum Electronics Conference, Monterey, CA, 23–25, April 2002*, IEEE, Piscataway, NJ, p. 24.
- <sup>7</sup>V. B. Neculaes, R. M. Gilgenbach, and Y. Y. Lau, *Appl. Phys. Lett.* **83**, 1938 (2003).
- <sup>8</sup>V. B. Neculaes, R. M. Gilgenbach, Y. Y. Lau, M. C. Jones, and W. M. White, *IEEE Trans. Plasma Sci.* **32**, 1152 (2004).
- <sup>9</sup>M. C. Jones, V. B. Neculaes, W. White, Y. Y. Lau, and R. M. Gilgenbach, *Appl. Phys. Lett.* **84**, 1016 (2004).
- <sup>10</sup>J. I. Kim, J. H. Won, and G. S. Park, *Appl. Phys. Lett.* **86**, 171501 (2005).
- <sup>11</sup>M. C. Jones, R. M. Gilgenbach, W. M. White, M. R. Lopez, V. B. Neculaes, and Y. Y. Lau, *Rev. Sci. Instrum.* **75**, 2976 (2004).
- <sup>12</sup>M. C. Jones, V. B. Neculaes, Y. Y. Lau, R. M. Gilgenbach, and W. M. White, *Appl. Phys. Lett.* **85**, 6332 (2004).
- <sup>13</sup>B. Goplan, L. Ludeking, D. Smithe, and G. Warren, *Comput. Phys. Commun.* **87**, 54 (1995).
- <sup>14</sup>V. B. Neculaes (unpublished, 2003).
- <sup>15</sup>M. C. Jones, Ph.D. dissertation, University of Michigan, April 2005.
- <sup>16</sup>M. Fuks and E. Schamiloglu, in *31st IEEE Conference on Plasma Science*, Baltimore, MD, June 2004.
- <sup>17</sup>J. W. Luginsland, Y. Y. Lau, V. B. Neculaes, R. M. Gilgenbach, M. C. Jones, M. H. Frese, and J. J. Watrous, *Appl. Phys. Lett.* **84**, 5425 (2004).
- <sup>18</sup>V. B. Neculaes, P. Pengvanich, Y. Hidaka, Y. Y. Lau, R. M. Gilgenbach, W. M. White, M. C. Jones, H. L. Bosman, and J. W. Luginsland, *IEEE Trans. Plasma Sci.* **33**, 654 (2005).